Nanoscale Res Lett (2009) 4:738–747
DOI 10.1007/s11671-009-9314-x

NANO EXPRESS

A Novel Approach to Molecular Recognition Surface of Magnetic Nanoparticles Based on Host–Guest Effect

Yuanpeng Wu · Fang Zuo · Zhaohui Zheng · Xiaobin Ding · Yuxing Peng

Received: 16 February 2009 / Accepted: 2 April 2009 / Published online: 23 April 2009

Abstract A novel route has been developed to prepared β-cyclodextrin (β-CD) functionalized magnetic nanoparticles (MNPs). The MNPs were first modified with monotosyl-poly(ethylene glycol) (PEG) silane and then tosyl units were displaced by amino-β-CD through the nucleophilic substitution reaction. The monotosyl-PEG silane was synthesized by modifying a PEG diol to form the corresponding monotosyl-PEG, followed by a reaction with 3-isocyanatopropyltriethoxysilane (IPTS). The success of the synthesis of the monotosyl-PEG silane was confirmed with ^{1}H NMR and Fourier transform infrared (FTIR) spectroscopy. The analysis of FTIR spectroscopy and X-ray photoelectron spectroscopy (XPS) confirmed the immobilization of β-CD onto MNPs. Transmission electron microscopy (TEM) indicated that the β-CD functionalized MNPs were mostly present as individual nonclustered units in water. The number of β-CD molecules immobilized on each MNP was about 240 according to the thermogravimetric analysis (TGA) results. The as-prepared β-CD functionalized MNPs were used to detect dopamine with the assistance of a magnet.

Keywords β-Cyclodextrin · Magnetic nanoparticles · Molecular recognition · Dopamine

Y. Wu · Z. Zheng · X. Ding (✉) · Y. Peng (✉)
Chengdu Institute of Organic Chemistry,
Chinese Academy of Sciences, Chengdu 610041,
People's Republic of China
e-mail: xbding@cioc.ac.cn

Y. Peng
e-mail: yxpeng@cdb.ac.cn

F. Zuo
Research Branch of Functional Materials,
State Key Laboratory of Electronic Films & Integrated Devices,
University of Electronic Science and Technology of China,
Chengdu 610054, People's Republic of China

Y. Wu
Graduate School of the Chinese Academy of Sciences,
Beijing 100049, People's Republic of China

Introduction

Molecular host–guest systems have captured much attention in recent years. By carefully selecting the host and guest molecules, specific properties of the resulting inclusion complexes can be targeted. Among a wide range of host molecules, an example of well-studied hosts would be the cyclodextrins (CDs) [1]. CDs are a group of naturally cyclic oligosaccharides, with six, seven, or eight glucose subunits linked by α-(1, 4) glycosidic bonds in a cylinder-shaped structure and are denominated as α-, β-, and γ-CD, respectively [2]. The inner surface of their molecular cavity is hydrophobic, because it is lined with the glycosidic oxygen bridges. Conversely, the outer surface of CD is hydrophilic due to the hydroxyl groups. They are able to form inclusion complexes with molecules that are hosted in the solute inner CD core due to interactions between hydrophobic moieties borne by these molecules and the internal surface of the CD cavity. It can bind a variety of guest molecules inside their torus-shaped cavities and serve as a model host site. For example, CD can form inclusion complexes with dopamine (DA) or uric acid (UA) through host–guest effect.

On the other hand, owing to containing two or more different functionalities, nanocomposites are attractive candidates for advanced nanomaterials. With controlled structure and interface interactions, these nanocomposites can exhibit novel physical and chemical properties that will

be essential for future technological applications. Recently, the functionalization of nanoparticle surfaces with macrocyclic host molecules in well-defined host–guest interactions has drawn considerable attention [3–25]. The combination of the physical properties of nanostructured materials and the molecular recognition ability of host molecules adsorbed on the nanoparticles surface makes them to exhibit promising applications in different fields such as catalysis [5–7], nanotechnology [8, 9], environment [10], chemical sensing [11–16], and so on. However, only a few cases concerning the bonding of CDs to nanoparticles have been investigated [5–10, 21–25]. At present, the research work on taking CD derivatives as capping ligands for nanoparticles is focused on the attachment of perthiolated CDs (SH-CDs) on metal nanoparticle surfaces. For instance, Liu et al. have reported the modification of gold [17–20], platinum [21], palladium [21–23], and CdSe-CdS [24] nanoparticles with SH-CDs. In addition, the work about the combination of CDs on the silica nanoparticles has also been reported [8].

Cyclodextrin-functionalized magnetic nanoparticles (MNPs) combining the properties of MNPs and the molecular recognition function of CD are expected to have multiple potential applications such as magnetic separation, medical diagnosis, and controlled drug delivery. Ohta and co-workers [26] inserted β-cyclodextrin (β-CD) derivatives onto the surface of MNPs by using self-assembly processes. However, to the best of our knowledge, there is no report about the binding of CD on the MNPs through the covalent binding. In this paper, we present a novel synthetic procedure for the synthesis of β-CD functionalized MNPs. First, a monotosyl-poly (ethylene glycol) (PEG) silane was prepared and then covalently bonded onto the surface of MNPs through the method which combines the ligand exchange reaction and condensation of the silane. Second, the tosyl termini of the PEG molecules which adsorbed on the MNPs were displaced by ethylenediamine-containing β-CD (EDA–β-CD) through the nucleophilic substitution reaction. And finally, the as-prepared β-CD functionalized MNPs were used to detect DA sensitively with the assistance of a magnet.

Experimental Section

Materials

β-Cyclodextrin (β-CD), ethylenediamine (EDA), $FeCl_3 \cdot 6H_2O$, $FeSO_4 \cdot 7H_2O$, oleic acid (OA), $NH_3 \cdot H_2O$, triethylamine (TEA), NaH_2PO_4, Na_2HPO_4, PEG (Mw = 1000 g/mol), toluene-4-sulfonyl-chloride (TsCl), KI, and Ag_2O were obtained from Sinopharm Chemical Reagent Co., Ltd. DA was purchased from Aldrich Co., Ltd. 3-Isocyanatopropyltriethoxysilane (IPTS) was obtained from Diamond Advanced Material of Chemical Inc. EDA–β-CD was prepared according to the already published procedure [27–29].

All other reagents were of analytical grade and were used without further purification.

All solutions were prepared with ultrapure water obtained from a water purification system (Millipore WR600A, Yamato Co., Japan). High purity nitrogen was used for solution deaeration prior to electrochemical measurements.

Synthesis of the Monotosyl-PEG Silane

The process and products for each reaction step are shown schematically in Scheme 1. First, the monotosyl-PEG was prepared [30]. In brief, to a chilled (0 °C) solution of the PEG (Mw = 1000 g/mol, 10.0 g; 10.0 mmol) in methylene

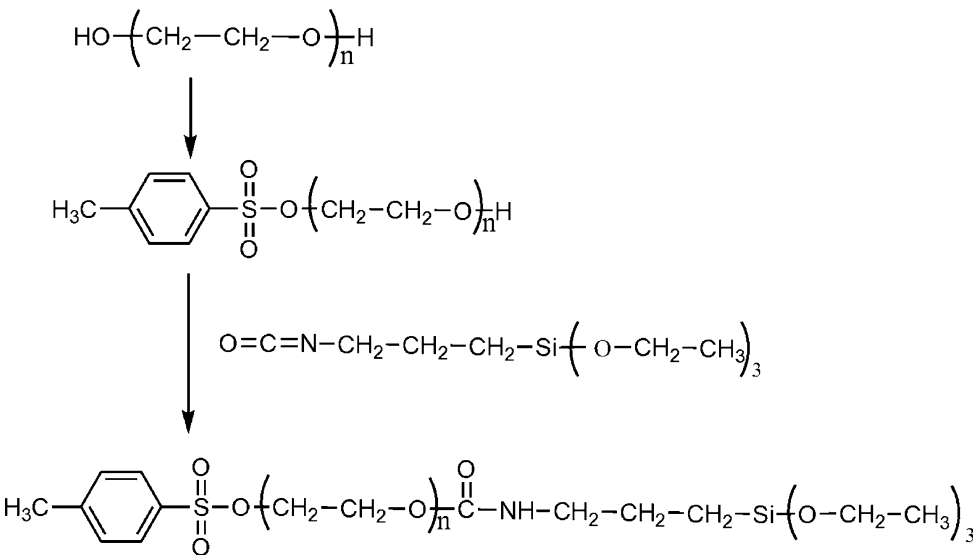

Scheme 1 Chemical scheme for the synthesis of the monotosyl-PEG silane

chloride (distilled, 160 mL), freshly prepared Ag_2O (1.50 equiv, 3.476 g; 15.0 mmol) and recrystallized KI (0.40 equiv, 664 mg; 4.0 mmol) were added. Then the purified TsCl (1.05 equiv, 2.0 g; 10.05 mmol) was dissolved in 20 mL methylene chloride, and the solution was added into the above PEG solution in one portion under rapid stir. The mixture was stirred continuously for 2 h under dry nitrogen. After the reaction, the mixture was carefully filtered over a pad of silica gel, and then the obtained clear filtrate was evaporated under reduced pressure to give a colorless oily product. The oily product was recrystallized (acetone/dry-ice bath) by using methylene chloride/ether mixture, and then monotosyl-PEG derivative was obtained as a white amorphous solid. Yield: 9.88 g (85%); ^{1}H NMR ($CDCl_3$, 300 MHz) δ7.76 (d, Ar), 7.31 (d, Ar), 4.15 (t, $\underline{CH_2}OTs$), 3.86–3.39 (m, CH_2), 3.12 (t, 2H, CH_2), 2.83 (t, 2H, CH_2), 2.63 (br, s, OH), 2.42 (s, Me tosyl).

Next, the monotosyl-PEG silane was synthesized from monotosyl-PEG and 3-IPTS using dibutyltin dilaurate as a catalyst. In brief, 5.8 g of dried monotosyl-PEG (5 mmol) was dissolved in 20 mL *N*,*N*-dimethylformamide (DMF). IPTS and dibutyltin dilaurate, a catalyst, were added to the monotosyl-PEG solution. The molar ratios of IPTS and dibutyltin dilaurate to monotosyl-PEG were 2.5 and 0.1, respectively. After adding chemical reagents, the mixture was stirred continuously for 6 h at 80 °C under dry nitrogen. After the reaction, the monotosyl-PEG silane was precipitated from DMF with cold diethyl ether twice and dried in vacuum. Yield: 5.5 g (81%); ^{1}H NMR ($CDCl_3$): δ7.76 (d, Ar), 7.31 (d, Ar), 5.05 (br, OC(O)$\underline{NH}$), 4.15 (t, $\underline{CH_2}OTs$), 4.09 (t, $\underline{CH_2}OC(O)NH$), 3.75 (t, $O\underline{CH_2}CH_3$), 3.53–3.82 (m, $(\underline{CH_2}\underline{CH_2}O)_n$), 3.08 (m, $\underline{CH_2}CH_2CH_2Si$), 2.42 (s, Me tosyl), 1.53 (m, $CH_2\underline{CH_2}CH_2Si$), 1.15 (t, $OCH_2\underline{CH_3}$), 0.54 (t, $\underline{CH_2}Si$).

Preparation of β-CD Functionalized MNPs

The β-CD functionalized MNPs were prepared according the approach shown in Scheme 2. OA-coated MNPs (OA–MNPs) were first synthesized via a two-step method [31, 32]. Then the monotosyl-PEG silane was immobilized on the MNPs. In a typical run, 50 mg monotosyl-PEG silane, 1.0 mL TEA (2 M in toluene), 10-mL toluene- and 5-mL toluene-based OA-MNPs dispersion were added into a 50-mL round-bottom flask. The mixture was stirred for 10 h at 50 °C and then at room temperature for 24 h under nitrogen atmosphere. Then, the resultant monotosyl-PEG immobilized nanoparticle precipitate was isolated by centrifugation after the addition of a small portion of diethyl ether, washed three times with dry toluene to remove the residual monotosyl-PEG silane and the displaced OA, and then dried in vacuum. Finally, MNPs were dispersed into DMF with content of 10 mg/mL.

In order to introduce β-CD on the MNPs, EDA–β-CD was used to react with the monotosyl termini of the PEG adsorbed on MNPs. In brief, 5-mL DMF based monotosyl-PEG–MNPs dispersion, 0.1 g EDA–β-CD, and 10-mL DMF were added into a 50-mL round-bottom flask. The mixture was stirred for 12 h at 70 °C. Then the resultant β-CD immobilized nanoparticle precipitate was isolated by centrifugation after the addition of a small portion of diethyl ether and washed three times with DMF to remove residual EDA–β-CD and then dried in vacuum. Finally, β-CD–PEG–MNPs were stored in DMF.

Electrochemical Experiment

Electrochemical measurements were performed on Arbin Instruments (MSTAT4+, USA) at room temperature (25 °C). A three-electrode single-compartment cell was used for cyclic voltammogram (CV). An Indium Tin Oxides (ITO, 1.0 cm^2) electrode was used as working electrode, a platinum wire as the counter electrode, and a saturated calomel electrode as the reference electrode. And all potentials were relative to the reference electrode. ITO was sonicated in 1:1 methylene chloride/acetone, rinsed thoroughly with ultrapure water, and then allowed to dry at room temperature under high purity nitrogen. A 0.1 mol L^{-1} phosphate buffer (pH 7.0) was used as an electrolyte solution. Phosphate buffer solution (0.1 mol L^{-1}) was prepared by mixing stock standard solutions of 0.1 mol L^{-1} Na_2HPO_4 and 0.1 mol L^{-1} NaH_2PO_4. And the concentration of DA was 1 mmol L^{-1}. A magnet of 1.1 T was used for absorbing the β-CD–PEG–MNPs from solution toward the ITO.

Instruments

^{1}H NMR spectra were measured on a JEOL JNM EX270 NMR spectrometer (300 MHz).

Fourier transform infrared (FTIR) spectra were measured on a Nicolet 200SXV-1 FTIR spectrometer. The acetone dispersion of MNPs was coated on the potassium bromide pellet.

X-ray photoelectron spectroscopy (XPS) was carried out on an XSAM-800 electron and take-off angle of 20° was used with X-ray source.

Transmission electron microscopy (TEM) was carried out on a JEM-100CX instrument operating an acceleration voltage of 80 kV. TEM specimens were prepared by aspirating an aqueous sample onto a copper EM grid.

Thermogravimetric analysis (TGA) was performed on a TA instrument Q50, at a scan rate of 10 °C/min. The temperature was from room temperature up to 800 °C under nitrogen atmosphere.

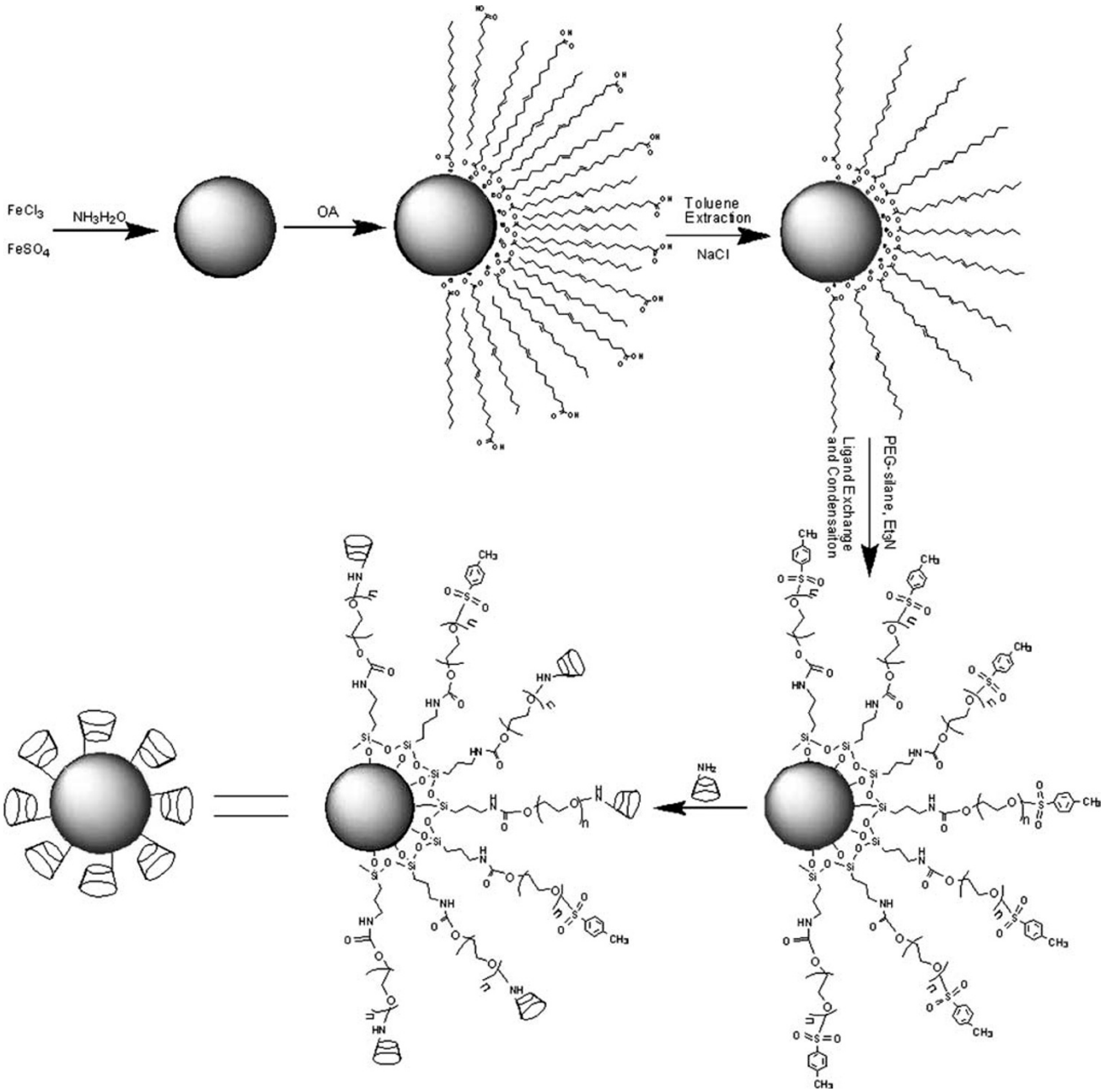

Scheme 2 Preparation of β-CD functionalized magnetic nanoparticles

Electrochemical measurements were performed on Arbin Instruments (MSTAT4+, USA) at room temperature.

Results and Discussion

Characterization of the Monotosyl-PEG Silane

In order to obtain the β-CD functionalized MNPs, a kind of monotosyl-PEG silane was first prepared as shown in Scheme 1. The PEG was converted to a monotosyl-PEG which reacted with IPTS to obtain the monotosyl-PEG silane. The structure of the monotosyl-PEG silane was identified by ^{1}H NMR analysis. The chemical shifts for protons from position 1 to 13 in the monotosyl-PEG silane are shown in Fig. 1 and in its inset table. The molecular structure of the monotosyl-PEG silane was confirmed by the presence of all the characteristic peaks and peak integration.

In order to further verify the successful synthesis of the monotosyl-PEG silane, FTIR spectra were also collected at each step of the synthesis, as shown in Fig. 2. The strong

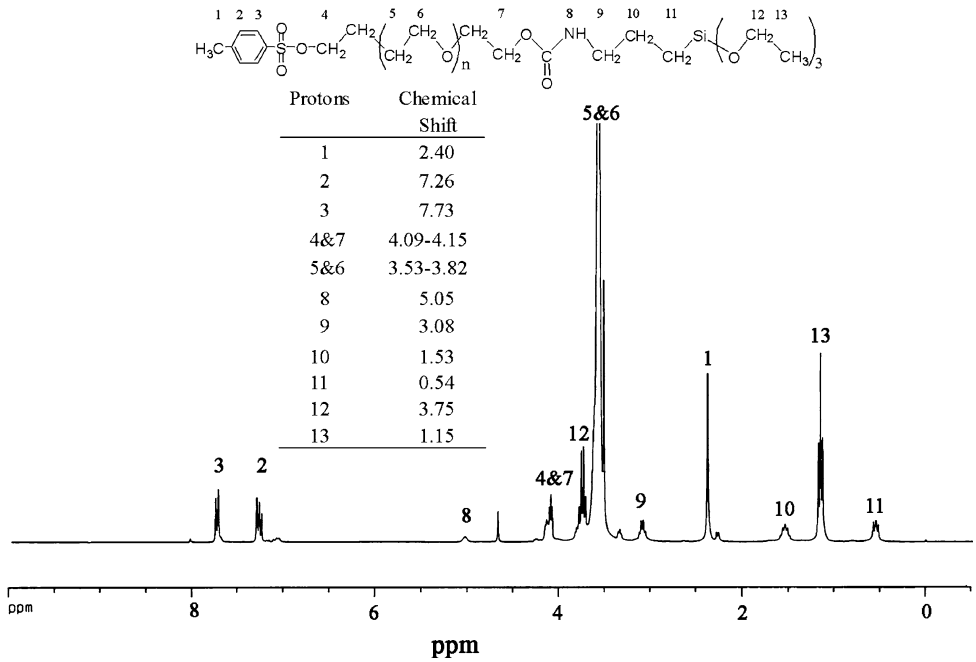

Fig. 1 ^{1}H NMR spectra of the monotosyl-PEG silane

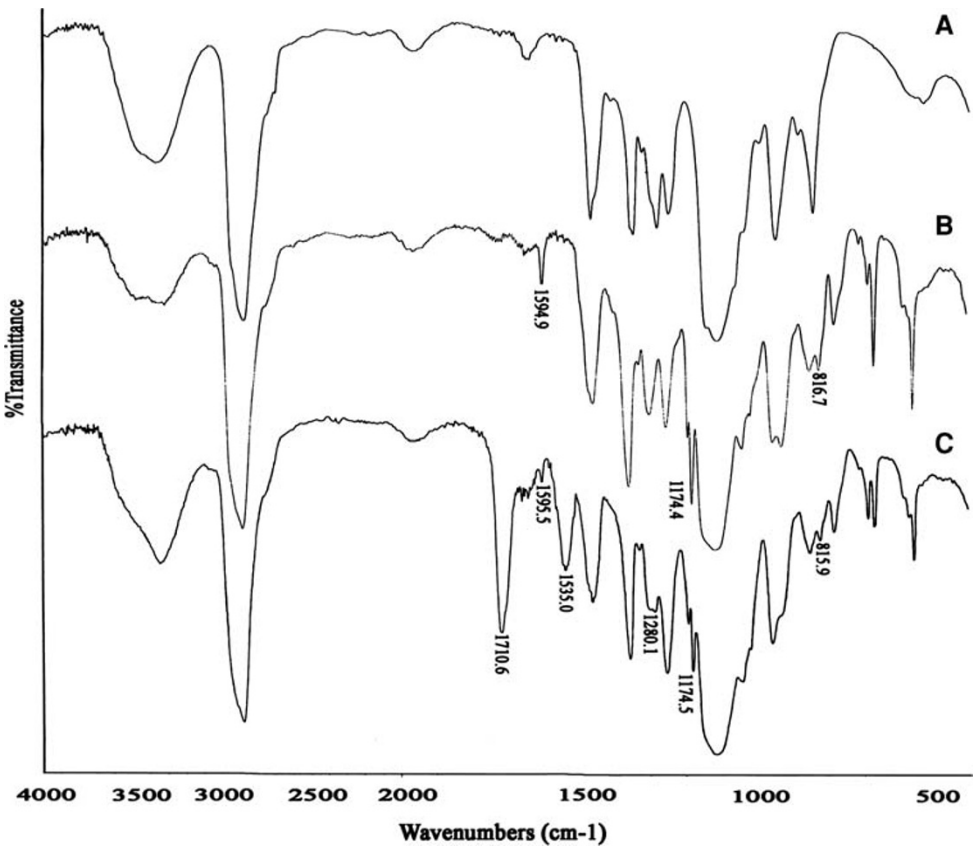

Fig. 2 FTIR spectra of (A) PEG, (B) monotosyl-PEG, and (C) monotosyl-PEG silane

absorption band at 1174.4 cm^{-1} in the monotosyl-PEG (Fig. 2b) was attributed to the stretching vibration of the tosyl termini of PEG. In addition, the appearance of the characteristic peak of the benzene ring vibration at 1594.9 cm^{-1} and the bending vibration of the benzene ring at 816.7 cm^{-1} also indicated that PEG had reacted with TsCl. The FTIR spectrum of the monotosyl-PEG silane (Fig. 2c) displays intense peaks at 1710.6 cm^{-1} corresponding to

C=O stretching vibration. The band at 1535.0 cm^{-1} resulted from the –NH bending vibration in the amide linkage between the silane and the PEG. Peak located at 1280.1 cm^{-1} is corresponding to Si–C stretching vibration.

Characterization of the MNPs

Once the synthesis of the monotosyl-PEG silane had been confirmed with ^{1}H NMR and FTIR spectroscopy, we immobilized the monotosyl-PEG silane on the MNPs following the scheme outlined in Scheme 2. FTIR spectra confirmed the successful surface modification as shown in Fig. 3. The disappearance of the 1560 and 1450 cm^{-1} bands belong to the presence of coordinated –COO– groups of OA adsorbed on OA–MNPs (Fig. 3a), and the appearance of the characteristic peaks of the PEG at 1250.6, 1098.3, and 1035.6 cm^{-1} (Fig. 3c) indicated the binding of PEG on the MNPs. In addition, the characteristic of benzene ring at 1596.2 and 815.9 cm^{-1} (Fig. 3c) confirmed the presence of the active tosyl-group on the surfaces of the modified MNPs.

In order to introduce β-CD onto the MNPs, the tosyl termini of PEG molecules which adsorbed on the MNPs was displaced by EDA–β-CD through the nucleophilic substitution reaction. Compared with the FTIR spectra of monotosyl-PEG–MNPs and EDA–β-CD as shown in Fig. 4, the characteristic peak of the α-pyranyl vibration of β-CD at 943.9 cm^{-1} appeared in the FTIR spectra of β-CD–PEG–MNPs (Fig. 4c). In addition, three most intense bands at 1151.2 cm^{-1} (antisymmetric stretching vibration of C–O–C glycosidic bridge), 1077.1 cm^{-1}, and 1028.7 cm^{-1} (coupled υ_S (C–C/C–O)) indicated the existence of β-CD. These data confirmed the successful introduction of β-CD onto the MNPs.

X-ray photoelectron spectroscopy was also applied to confirm the modification of MNPs. Contributions from the ether carbon component at 286.5 eV was observed in the C1s peaks of the monotosyl-PEG–MNPs (Fig. 5a), which provided clear evidence of PEG on the MNPs surfaces. Compared with that on the monotosyl-PEG–MNPs, the peak area of C–O (286.10 eV) on the β-CD–PEG–MNPs (Fig. 5b) was increased, and at the same time a new peak of O–C–O (287.05 eV) was observed. Undoubtedly, therefore, it could be concluded that β-CD was adsorbed on the surfaces of MNPs.

The morphology of the β-CD–PEG–MNPs dispersed in water revealed by TEM was shown in Fig. 6. The TEM micrograph indicated that the β-CD–PEG–MNPs are highly dispersed. The average particle sizes were about 11.0 nm.

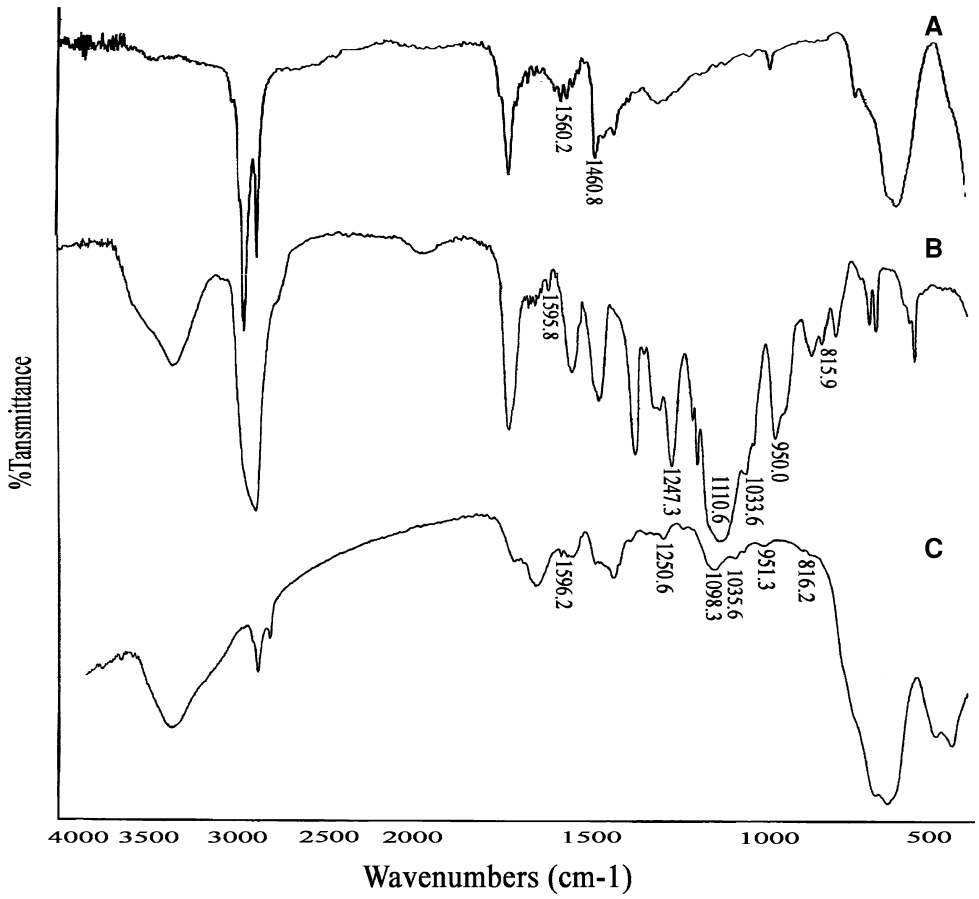

Fig. 3 FTIR spectra of (A) OA–MNPs, (B) pure monotosyl-PEG silane, and (C) monotosyl-PEG–MNPs

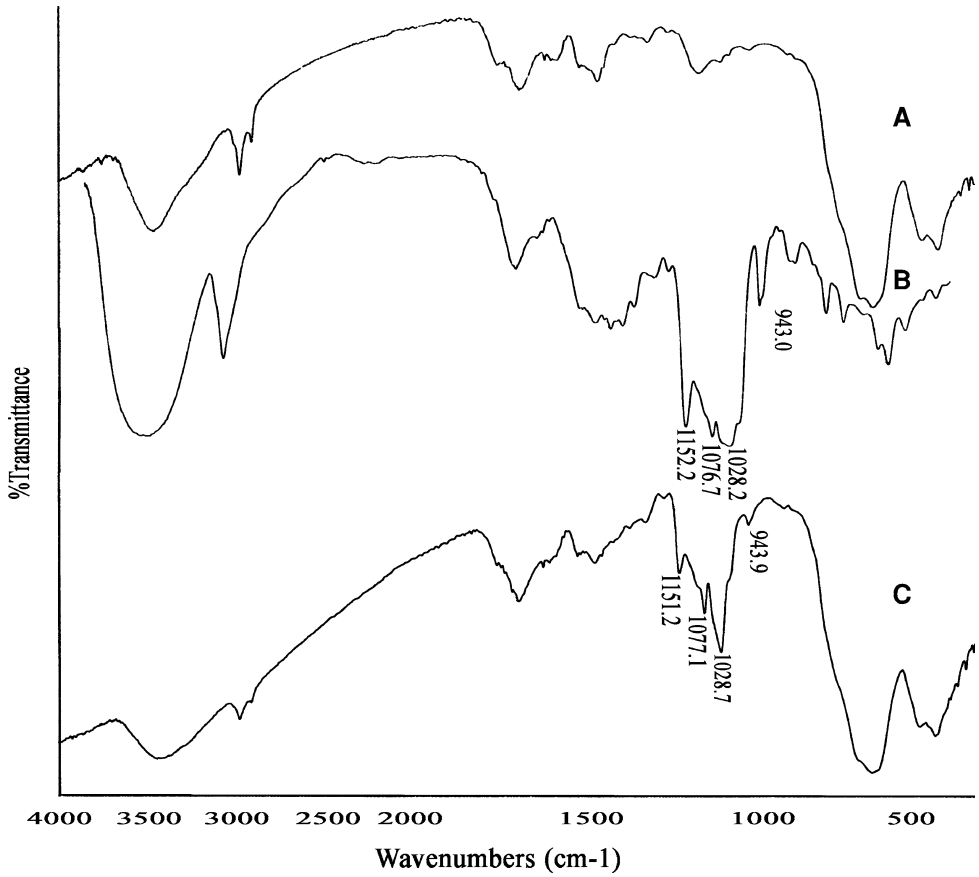

Fig. 4 FTIR spectra of (A) monotosyl-PEG–MNPs, (B) pure EDA–β-CD, and (C) β-CD–PEG–MNPs

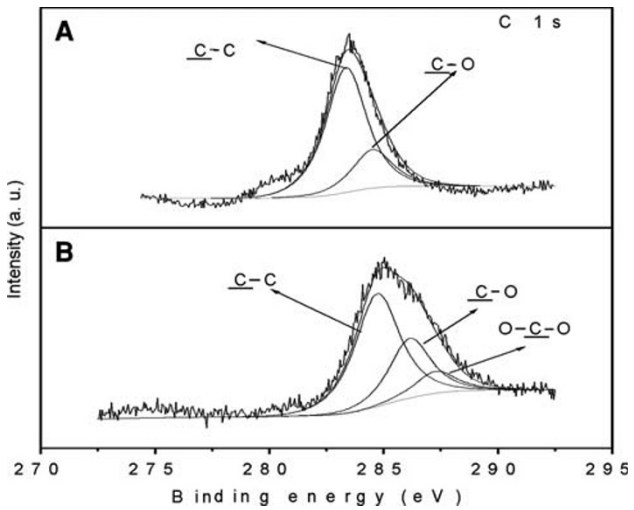

Fig. 5 XPS spectra of **a** monotosyl-PEG–MNPs and **b** β-CD–PEG–MNPs

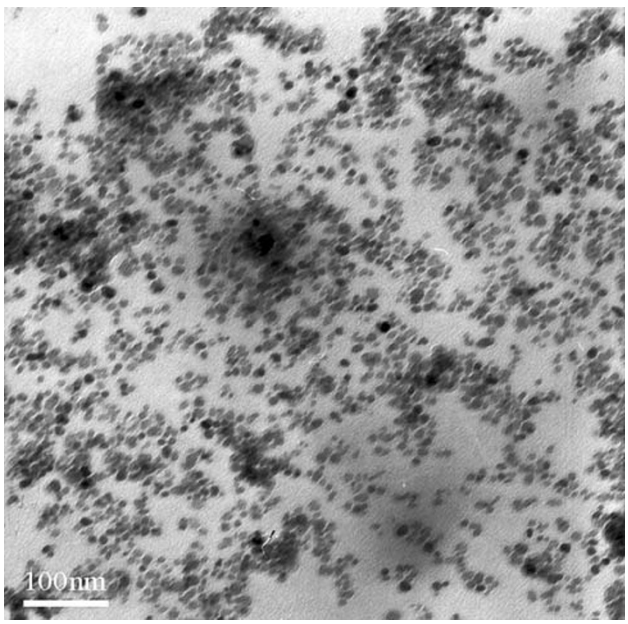

Fig. 6 TEM micrograph of β-CD–PEG–MNPs

The substitution percent (%SP) of the tosyl termini of the monotosyl-PEG molecules which adsorbed on the MNPs by EDA–β-CD and the number of β-CD molecules immobilized on a single MNP were determined by TGA. The monotosyl-PEG–MNPs were first analyzed to measure the amount of adsorbed PEG present before the introduction of β-CD. The weight loss of the monotosyl-PEG–MNPs is quite small below 100 °C, moderate up to 185 °C, but significant at temperatures higher than 180 °C (Fig. 7a). PEG with low Mw (550 and 5000) can be

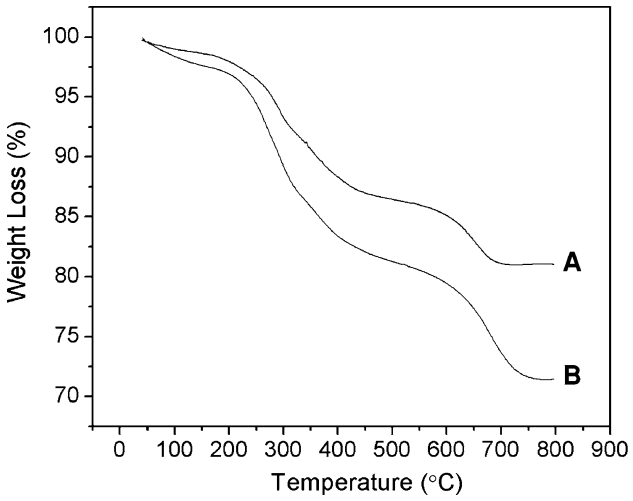

Fig. 7 TGA spectrum of (A) monotosyl-PEG–MNPs and (B) β-CD–PEG–MNPs

degraded at about 280 °C [33]. According to the TGA data, the main weight loss is observed at about 310 °C. The amount of monotoysl-PEG coated on the surface of the MNPs could be calculated on the basis of the TGA data and was found to be 17.1 wt% of the mass of the monotosyl-PEG–MNPs. Compared with that of the monotosyl-PEG–MNPs, the weight loss of β-CD–PEG–MNPs was 26.3 wt% (Fig. 7b). The increase of the weight loss is ascribed to the β-CD immobilized on the MNPs. The %SP could be calculated using formula (1), where W_{CD} and W_{PEG} are the weight loss of the β-CD–PEG–MNPs and the monotosyl-PEG–MNPs, respectively; M_{CD} and M_{PEG} are the molar mass of the β-CD immobilized on the β-CD–PEG–MNPs and the molar mass of the monotosyl-PEG immobilized on the monotosyl-PEG–MNPs, respectively. Taking into account the displaced tosyl chloride, the value of 0.868 was given in formula (1). The %SP being calculated was 69.1%, that is to say, not all the tosyl termini reacted with EDA–β-CD. This behavior was due to the wrapping effect of the long chain of PEG which avoided the reaction between tosyl termini and EDA–β-CD.

$$\%\mathrm{SP} = \frac{(W_{CD} - W_{PEG})/0.868M_{CD}}{W_{PEG}/M_{PEG}}. \quad (1)$$

In addition, according to formula (2), the number of β-CD molecules immobilized on a single MNP could be calculated, where N is the number of β-CD molecules immobilized on each MNP, R is the mean radius of the β-CD–PEG–MNPs (5.5 nm based on TEM results), ρ is the density of the nanoparticles (5.18 g/cm^3), N_A is Avogadro's number. The number of β-CD molecules immobilized on each β-CD–PEG–MNP being calculated was about 240.

$$N = \frac{4 \times (W_{CD} - W_{PEG})N_A\rho\pi R^3}{0.86 \times M_{CD}(1 - W_{CD}) \times 3 \times 10^{21}}. \quad (2)$$

Application of β-CD–PEG–MNPs in the Detection of DA

DA is an important neurotransmitter in mammalian central nervous systems. Changes in DA levels are related to neurological disorders, such as schizophrenia, Parkinson's disease, and to HIV infection [34]. Therefore, determination of DA is important and has attracted much attention from neuroscientists and chemists. As a guest molecule, DA can form inclusion complexes with β-CD due to hydrophobic and hydrogen-bonding interaction [35]. In the present article, the as-prepared β-CD–PEG–MNPs were used to detect DA through two steps (Fig. 8A). First,

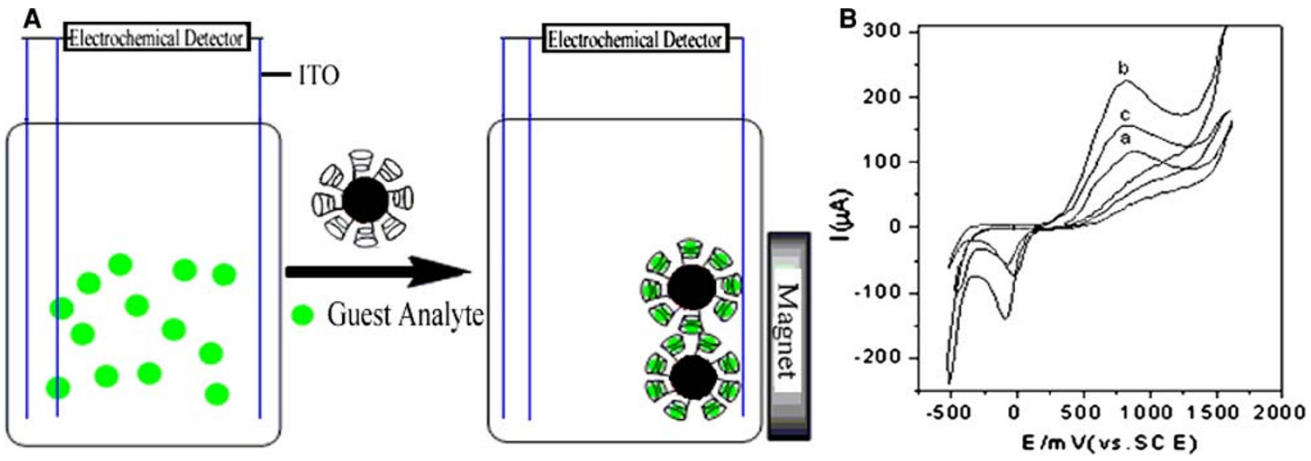

Fig. 8 **A** Schematic illustration of magnet controlled electrochemical detection of DA. **B** CVs of 1.0 mM DA in phosphate buffer solution (0.1 M) without MNP (a), addition of TS–PEG–MNP and adsorbed onto the surface of ITO by a magnet (b), addition of β-CD–PEG–MNP and adsorbed onto the surface of ITO by a magnet (c). Potential scan rate: 100 mV s^{-1}

β-CD–PEG–MNPs were dispersed in aqueous solution containing DA. After a few minutes, DA molecules were absorbed on the surface of MNPs through molecular recognition interaction between DA and β-CD. Second, the MNPs were absorbed onto ITO by using an exterior magnet for the electrochemical detection of DA.

Figure 8B(a) shows the CV of 1.0 mM DA in 0.1 M phosphate buffer solution (pH 7) at ITO. TS–PEG–MNPs were added to the electrolyte solution containing 1.0 mM DA. Then the MNPs were absorbed onto ITO by using a magnet and the CV was obtained (Fig. 8B(b)). The oxidation peak current enhanced obviously by comparing curve b with curve a. This behavior is attributed to the electrocatalytic effect of MNPs [36]. In another experiment, β-CD–PEG–MNPs were added to the electrolyte solution containing 1.0 mM DA and stirred for 10 min. Then β-CD–PEG–MNPs were absorbed onto ITO by an exterior magnet and the CV was obtained (Fig. 8B(c)). The oxidation peak current is higher than curve b. This result must be in accordance with the fact that the DA apparent concentration in curve c is much higher than the bulk concentration owing to the formation of inclusion complex between β-CD and DA [37]. Therefore, due to both the electrocatalytic effect of MNPs and host–guest effect of β-CD to DA, β-CD–PEG–MNPs modified electrode can detect DA sensitivity with the assistance of an exterior magnet.

Conclusion

In summary, a simple and straightforward synthetic method has been developed for the preparation of β-CD functionalized MNPs that combine magnetic and molecular recognition properties. Various techniques have been utilized to characterize the β-CD functionalized MNPs, and the results showed the desired properties as designed. Its application in magnetic responsive detecting of DA has been demonstrated well. And its detailed application in sensor is under research.

Acknowledgments This work was financially supported by the National Nature Science Foundation of China (No. 50673091) and the Nature Science Foundation of Jiangsu Province, China (No. BK20080668).

References

1. G. Wenz, B. Han, A. Moller, Chem. Rev. **106**, 782 (2006). doi:10.1021/cr970027+
2. M.T. Rojas, R. Kiiniger, J.F. Stoddart, A.E. Kaifer, J. Am. Chem. Soc. **117**, 336 (1995). doi:10.1021/ja00106a036
3. R. Tshikhudo, D. Demuru, Z. Wang, M. Brust, A. Secchi, A. Arduini, A. Pochini, Angew. Chem. Int. Ed. **44**, 2913 (2005). doi:10.1002/anie.200462909
4. M.L. Ben-Ishay, A. Gedanken, Langmuir **23**, 5238 (2007). doi:10.1021/la0633076
5. M. Kawamura, K. Sato, Chem. Commun. (Camb.) **32**, 3404 (2007). doi:10.1039/b705640k
6. R. Villalonga, R. Caob, A. Fragoso, A.E. Damiao, P.D. Ortiz, J. Caballero, J. Mol. Catal. B Enzym. **35**, 79 (2005). doi:10.1016/j.molcatb.2005.06.002
7. L. Li, X. Sun, Y. Yang, N. Guan, F. Zhang, Chem. Asian J. **1**, 664 (2006). doi:10.1002/asia.200600103
8. V. Mahalingam, S. Onclin, M. Peter, B.J. Ravoo, J. Huskens, D.N. Reinhoudt, Langmuir **20**, 11756 (2004). doi:10.1021/la047982w
9. P. Maury, M. Peter, O. Crespo-Biel, X.Y. Ling, D.N. Reinhoudt, J. Huskens, Nanotechnology **18**, 1 (2007). doi:10.1088/0957-4484/18/4/044007
10. R. Sawicki, L. Cier, Environ. Sci. Technol. **40**, 1978 (2006). doi:10.1021/es051441r
11. S.Y. Lin, S.W. Liu, C.M. Lin, C. Chen, Anal. Chem. **74**, 330 (2002). doi:10.1021/ac0156316
12. A. Arduini, D. Demuru, A. Pochini, A. Secchi, Chem. Commun. (Camb.) **5**, 645 (2005). doi:10.1039/b411883a
13. H. Li, Y. Zhang, X. Wang, D. Xiong, Y. Bai, Mater. Lett. **61**, 1474 (2007). doi:10.1016/j.matlet.2006.07.064
14. P. Leyton, S. Sanchez-Cortes, J. Garcia-Ramos, M. Campos-Vallette, J. Phys. Chem. B **108**, 17484 (2004). doi:10.1021/jp047949i
15. H. Li, F. Qu, Chem. Mater. **19**, 4148 (2007). doi:10.1021/cm0700089
16. L. Guerrini, J.V. Garcia-Ramos, C. Domingo, S. Sanchez-Cortes, Langmuir **22**, 10924 (2006). doi:10.1021/la062266a
17. J. Liu, S. Mendoza, E. Roman, M.J. Lynn, R. Xu, A.E. Kaifer, J. Am. Chem. Soc. **121**, 4304 (1999). doi:10.1021/ja990330n
18. J. Liu, W. Ong, E. Roman, M.J. Lynn, A.E. Kaifer, Langmuir **16**, 3000 (2000). doi:10.1021/la991519f
19. J. Liu, J. Alvarez, W. Ong, E. Roman, A.E. Kaifer, Nano Lett. **1**, 57 (2001). doi:10.1021/nl0001813
20. J. Liu, J. Alvarez, W. Ong, E. Roman, A.E. Kaifer, J. Am. Chem. Soc. **123**, 11148 (2001). doi:10.1021/ja003957a
21. J. Alvarez, J. Liu, E. Roman, A.E. Kaifer, Chem. Commun. (Camb.) **13**, 1151 (2000). doi:10.1039/b002423f
22. J. Liu, J. Alvarez, W. Ong, E. Roman, A.E. Kaifer, Langmuir **17**, 6762 (2001). doi:10.1021/la015563i
23. L. Strimbu, J. Liu, A.E. Kaifer, Langmuir **19**, 483 (2003). doi:10.1021/la026550n
24. K. Palaniappan, C. Xue, G. Arumugam, S.A. Hackney, J. Liu, Chem. Mater. **18**, 1275 (2006). doi:10.1021/cm051602q
25. G.W. Diao, C. Qian, M. Chen, Y.J. Huang, Supramol. Chem. **18**, 117 (2006). doi:10.1080/10610270500467758
26. Y.L. Hou, H. Kondoh, M. Shimojo, E.O. Sako, N. Ozaki, T. Kogure, T. Ohta, J. Phys. Chem. B **109**, 4845 (2005). doi:10.1021/jp0476646
27. R.C. Petter, J.S. Salek, C.T. Sikorski, G. Kumaravel, F.T. Lin, J. Am. Chem. Soc. **112**, 3860 (1990). doi:10.1021/ja00166a021
28. Y.Y. Liu, X.D. Fan, L. Gao, Macromol. Biosci. **3**, 715 (2003). doi:10.1002/mabi.200300052
29. Y.Y. Liu, X.D. Fan, Biomaterials **26**, 6367 (2005). doi:10.1016/j.biomaterials.2005.04.011
30. I. Shenoy, W. Fu, J. Li, G. Jones, C. Dimarzio, S. Sridhar, M. Amiji, Int. J. Nanomed. **1**, 51 (2006). doi:10.2147/nano.2006.1.1.51
31. Y.B. Sun, X.B. Ding, Z.H. Zheng, X. Cheng, X.H. Hu, Y.X. Peng, Macromol. Rapid Commun. **28**, 346 (2007). doi:10.1002/marc.200600727
32. Y.B. Sun, X.B. Ding, Z.H. Zheng, X. Cheng, X.H. Hu, Y.X. Peng, Eur. Polym. J. **43**, 762 (2007). doi:10.1016/j.eurpolymj.2006.10.021

33. C.G. Granqvist, R.H. Buhrman, J. Appl. Phys. **47**, 2200 (1976). doi:10.1063/1.322870
34. J.W. Mo, B. Ogorevc, Anal. Chem. **73**, 1196 (2001). doi:10.1021/ac0010882
35. T.J. Yin, W.Z. Wei, J.X. Zeng, Anal. Bioanal. Chem. **386**, 2087 (2006). doi:10.1007/s00216-006-0845-z
36. B. Fang, G. Wang, W. Zhang, M. Li, X. Kan, Electroanalysis **17**, 744 (2005). doi:10.1002/elan.200403136
37. S.G. Wu, T.L. Wang, Z.Y. Gao, H.H. Xu, B.N. Zhou, C.Q. Wang, Biosens. Bioelectron. **23**, 1776 (2008). doi:10.1016/j.bios.2008.02.012